

**Received:** 09 July, 2025

**Accepted:** 28 July, 2025

**Published:** 29 July, 2025

**\*Corresponding author:** Nandigana VR Vishal, 206 Fluids Systems Laboratory, Department of Mechanical Engineering, Indian Institute of Technology Madras, Chennai 600036, Tamil Nadu, India, E-mail: [nandiga@zmail.iitm.ac.in](mailto:nandiga@zmail.iitm.ac.in)

**Keywords:** Nanopores; Conical nanopores; Membranes; Noise and Simulation

**Copyright License:** © 2025 Vishal NVR. This is an open-access article distributed under the terms of the Creative Commons Attribution License, which permits unrestricted use, distribution, and reproduction in any medium, provided the original author and source are credited.

<https://www.mathematicsgroup.us>



Check for updates

## Review Article

# Ion Transport, Current–noise in Nanopores and Conical Nanopores

**Nandigana VR Vishal\***

206 Fluids Systems Laboratory, Department of Mechanical Engineering, Indian Institute of Technology Madras, Chennai 600036, Tamil Nadu, India

## Abstract

In this paper, we build an ion transport model that requires less computational cost. We study the ion transport firstly in conical nanopores. We study the current-time in conical nanopores. The noise is modelled in our study. The noise in conical nanopores is due to the pore diameter and salt concentration. We consider 1 M KCl. We extend our study to understand the current time in nanopores. We consider the graphene nanopores. The noise in our nanopores model is due to the pore diameter only. We consider 1 M KCl. We study the influence of ion transport from the conductance relation to concentration for the solid-state nanopores. The concentrations studied are 0.003 M, 0.01 M, 0.03 M, 0.05 M, 0.15 M, 0.3 M, 0.4 M, 0.5 M, and 1 M KCl. We study the linear current-voltage characteristics for solid-state nanopores. We consider 1 M KCl. The study of nanofluidics can find applications in energy, water desalination, and neuromorphic computing devices.

## 1. Introduction

Nanofluidics is the study and manipulation of fluids confined within 1–100 nm. [1–3]. Nanofluidics involves the control, manipulation, and transport of fluids inside the nanopore. The physics observed inside nanopore structures is not observed in larger micro and bulk structures. The electrolyte solution used is KCl [4–7] and sodium phosphate made from sodium phosphate monobasic monohydrate  $\text{NaH}_2\text{PO}_4$  and sodium phosphate dibasic heptahydrate  $\text{Na}_2\text{HPO}_4$  [8,9]. The ion transport is studied by applying a voltage and measuring the ionic current in a single nanopore or nanopores. The nanopore surface has a negative charge contributed by the surface potential of the nanoporous membrane [10]. Under the application of voltage, the ion transport inside the nanopore is dominated by the surface interaction of the nanopore and its volume. The ratio of surface area to volume is large inside the nanopores. This results in a larger electrostatic force on the transport inside the nanopores. The surface of the nanopore parameters are surface charge density, material, and surface potential. The parameters have recently been explored in detail from the visual relation

to the pore geometry [11]. The behaviour of fluid changes at the nanoscale compared to the bulk scale, because atomic and molecular interactions between solid–liquid interfaces play a significant role at such small length scales. In recent studies, there is a focus on single and multiple nanopore membranes to understand the ionic current–time. However, the solid–state nanopores have significantly higher noise than the biological membranes. There are different nanopore membrane materials silicon nitride sputtered with silicon dioxide [12], graphene [13], and molybdenum disulfide ( $\text{MoS}_2$ ) [14]. The conical nanopores are being researched to understand the ion transport. The conical nanopores rectify the ion transport. Thus, the ion current is higher for voltages applied and their one direction compared to polarity change of the voltage and its direction. The polarity change of the voltage and direction inside the conical nanopores results in lower current [15]. Nowadays, new research on conical nanopores is towards understanding how to build computing technology [16].

Here we study the current–time oscillations inside the conical nanopores. We develop an oscillation numerical model

to understand the ion transport in the conical nanopores. We study the noise in the current inside the conical nanopores. In our oscillation model, we take into consideration the charge term, electrokinetic term, thermal current noise, and charge carrier noise to obtain the current-time oscillations inside the conical nanopores. Here we study the current-time oscillations inside the nanopores. We study graphene nanopores. Graphene has no negative surface charge on the walls of the nanopore. We study the noise in the current inside the nanopores. We measure the Power Spectral Density (PSD) from ionic current-time oscillations inside the nanopores. There is 1/f noise in the nanopores. The reason for the 1/f noise and current oscillations inside the nanopores is are pore diameter only. Further, we study the conductance as a function of concentration inside the nanopores. Furthermore, we study the linear current-voltage relationship inside the nanopores. The nanofluidics can find applications in single-molecule sensing, electrokinetic pumps, preconcentration of analytes using electric field focusing, water desalination, energy storage, energy, and memristor neuromorphic computing applications.

## 2. Theory

### Steady-state ion current calculations for the conical nanopore

The volume of the conical nanopore is given by Eq. (1)

$$V_{cn} = \frac{\pi L_{cn}}{3} (R^2 + Rr + r^2) \quad (1)$$

Where  $V_{cn}$  is the volume of the conical nanopore,  $R$  is the large radius, and  $r$  is the small radius.  $L_{cn}$  is the thickness of the conical nanopore. Here, the small radius is 2.5 nm and the large radius is 150 nm. The thickness of the conical nanopore is 12  $\mu\text{m}$  [15]. The volume of the conical nanopore is  $V_{cn} = 2.9 \times 10^{-19} \text{ m}^3$ . We consider the voltage to be 0.85 V. We consider a 1 M KCl concentration. The conical nanopore parameters are given in Tables 1,2, respectively.

The steady state ion current in the conical nanopore is given by Eq. (2).

$$I = \frac{qu}{L_{cn}} + \frac{mau}{\phi} \quad (2)$$

where  $q$  is the charge of KCl,  $u$  is the velocity,  $m$  is the mass of KCl,  $a$  is the acceleration of KCl, and  $\phi$  is the electric potential in the conical nanopore. We consider equal contribution of steady state current due to potassium ions ( $I^{K^+}$ ) and chlorine ions ( $I^{Cl^-}$ ).

**Table 1:** Conical nanopore list 1 model parameters.

$\phi$ (V)	$V_{cn}$ ( $\text{m}^3$ )	$c^{K^+}$ (mM)	$c^{Cl^-}$ (mM)	$m^{K^+}$ (kg)	$m^{Cl^-}$ (kg)	$q^{K^+}$ (C)	$q^{Cl^-}$ (C)
0.85	2.90E-19	1000	1000	1.25e-3	1.25e-3	2.8e-11	2.8e-11

**Table 2:** Conical nanopore list 2 model parameters.

$u$ (m/s)	$a$ ( $\text{m/s}^2$ )	$I^{K^+}$ (A)	$I^{Cl^-}$ (A)	$I$ (A)	$I$ (A) (experiment)
1e-04	1e-03	3.74E-10	3.74E-10	7.6E-10	7.65E-10

The steady-state potassium ion current in the conical nanopore is given by Eq. (3).

$$I^{K^+} = \frac{q^{K^+} u}{L_{cn}} + \frac{m^{K^+} au}{\phi} \quad (3)$$

where  $I^{K^+}$  is the potassium ion current,  $q^{K^+}$  is the charge of the potassium ion, and  $m^{K^+}$  is the mass of the potassium ion.

The steady state chlorine ion current in the conical nanopore is given by Eq. (4).

$$I^{Cl^-} = \frac{q^{Cl^-} u}{L_{cn}} + \frac{m^{Cl^-} au}{\phi} \quad (4)$$

where  $I^{Cl^-}$  is the chlorine ion current,  $q^{Cl^-}$  is the charge of the chlorine ion, and  $m^{Cl^-}$  is the mass of the chlorine ion.

The steady-state ion current in the conical nanopore is given.

$$I = I^{K^+} + I^{Cl^-}$$

In the numerical model, the current from the concentration calculated charge contributes 64%. The reason for the oscillations in the experiments was due to the pore diameter and salt concentration. The evidence in the experiments directly showed the role of salt concentration.

We show the concentration of potassium calculated charge and their current given by the term charge current  $\frac{q^{K^+} u}{L_{cn}}$  is high in the potassium ion current Eq (3) for conical geometry nanopore. We understand the current in a conical nanopore has an electrokinetic contribution from the potential, potassium ion migration, and convective components. This is presented in our numerical simulation for a conical nanopore. The term is  $\frac{m^{K^+} au}{\phi}$  that contributes to 36% of the potassium ion current in the conical nanopore.

We show the concentration of chlorine calculated charge and their current given by the term charge current  $\frac{q^{Cl^-} u}{L_{cn}}$  is high (64%) in the chlorine ion current Eq (4) for conical geometry nanopore. We understand the current in a conical nanopore has an electrokinetic contribution from the potential, chlorine ion migration, and convective components. This is presented in our numerical simulation for a conical nanopore.

The term is  $\frac{m^{Cl^-} au}{\phi}$  that contributes to 36% of the chlorine ion current in the conical nanopore. Earlier works are usually COMSOL, OpenFOAM, and molecular dynamics software. Our model reduces the computational cost by capturing the effects of the influence of conical nanopore geometry by volume. We consider the electrokinetic convective contribution, electric potential, KCl individual potassium ion migration, chlorine ion migration, and charge transport. In order to understand the current oscillations, we go in-depth on the current-time signal [15]. In our analysis, we consider the time step to be 1 s.

### 3. Results and discussion

#### Current oscillations of the conical nanopore, high-frequency thermal current noise

The high-frequency thermal current noise is given in Eq. (5).

$$I_{high} = \sqrt{4kG_{cn}TB} \quad (5)$$

where  $I_{high}$  is the high-frequency thermal current noise,  $k$  is the Boltzmann constant,  $G_{cn}$  is the conductance of the conical nanopore,  $T$  is the temperature, and  $B$  is the frequency bandwidth in Hz.

The conductance ( $G_{cn}$ ) of the conical nanopore is obtained from Eq. (6).

$$G_{cn} = \frac{I}{\phi} \quad (6)$$

Using Eq. (6), we obtain that the conductance in the conical nanopore is 894 pS. The high-frequency thermal current noise is given in Eq. (5). The value of the high-frequency thermal current noise is small [17].

#### Low-frequency charge carrier current noise

The low-frequency charge carrier current noise is given in Eq. (7).

$$I_{low} = A_{cn}f_L \quad (7)$$

where  $I_{low}$  is the low-frequency charge carrier current noise.  $A_{cn}$  is the noise property defined by the conical pore, small and large diameters. Further, the noise property is related to KCl concentration given in Eq. (8).  $f_L$  is the low-frequency term given in Eq. (9). We consider KCl concentration to be 2000 mM [15].

$$A_{cn} = \alpha c_{KCl} F V_{cn} \quad (8)$$

where  $\alpha$  is the fitting parameter ( $\alpha = 0.36$ ). The noise property is 20 pC.

$$f_L = 1/t_L \quad (9)$$

where  $t_L$  is the time 1s to calculate the low-frequency noise. The noise property  $A_{cn}$ , we call the charge carrier term. The noise property  $A_{cn}$  is fixed and oscillates every second, where the frequency ( $f_L$ ) is 1 Hz. The contribution of the low-frequency charge carrier current noise and high-frequency thermal current noise to the current inside the conical nanopore is given in Eq. (10).

$$I_{cn} = \begin{cases} I + I_{high} - I_{low}; & \text{oscillation 1} \\ I + I_{high} + I_{low}; & \text{oscillation 2} \end{cases} \quad (10)$$

Where  $I_{cn}$  are the ion current inside the conical nanopore that captures the oscillations. Figure 1 shows the current inside the conical nanopore that matches the literature [15].

#### 3.1 Steady-state ion current calculations for the nanopore

The volume of the nanopore is given by Eq. (11)

$$V_{np} = \pi R_{np}^2 L_{np} \quad (11)$$

where  $V_{np}$  is the volume of the nanopore,  $R_{np}$  is the radius of the nanopore, and  $L_{np}$  is the thickness of the nanopore. In this study, the radius is 5 nm and the thickness of the nanopore is 0.34 nm. We study the graphene nanopore in our model [13]. The volume of the nanopore is  $V_{np} = 2.7 \times 10^{-26} \text{ m}^3$ . The voltage is 0.1 V. We consider 1M KCl. The nanopore parameters are given in Tables 3,4, respectively.

The steady state ion current in the nanopore ( $I_{np}$ ) is given by Eq. (12).

$$I_{np} = \frac{qu}{L_{np}} + \frac{mau}{\phi} \quad (12)$$

where  $q$  is the charge of KCl,  $u$  is the velocity,  $m$  is the mass of KCl,  $a$  is the acceleration of KCl, and  $\phi$  is the electric potential in the nanopore. We consider equal contribution of steady state current to potassium ions ( $I^{K^+}$ ) and chlorine ions ( $I^{Cl^-}$ ).

The steady-state potassium ion current in the nanopore is given by Eq. (13).

$$I^{K^+} = \frac{q^{K^+}u}{L_{np}} + \frac{m^{K^+}au}{\phi} \quad (13)$$

where  $I^{K^+}$  is the potassium ion current,  $q^{K^+}$  is the charge of the potassium ion, and  $m^{K^+}$  is the mass of the potassium ion.

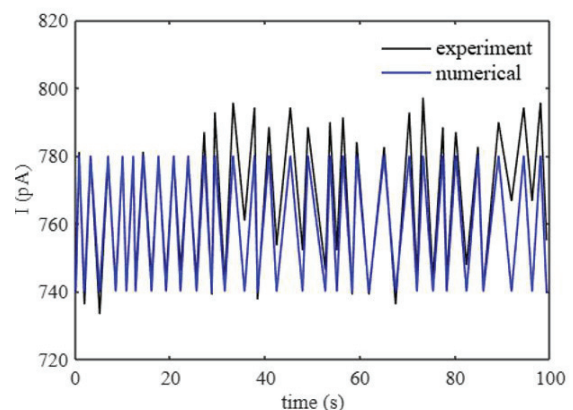


Figure 1: Current oscillations of a conical nanopore. The experiment results of the conical nanopore are in [15].

Table 3: The nanopore list 1 model parameters. The concentration of KCl is 1M.

$\phi(V)$	$V_{np}(\text{m}^3)$	$c^{Cl^-}(\text{mM})$	$m^{K^+}(\text{kg})$	$m^{Cl^-}(\text{kg})$	$q^{K^+}(C)$	$q^{Cl^-}(C)$	$q^{Cl^-}(C)$
0.1	$2.7 \times 10^{-26}$	1000	1000	4e-3	4e-3	2.58e-18	2.58e-18

Table 4: The nanopore list 2 model parameters. The concentration of KCl is 1M.

$v(\text{m/s})$	$a(\text{m/s}^2)$	$I^{K^+}(A)$	$I^{Cl^-}(A)$	$I(A)$	$I(A)$ (experiment)
1e-04	1e-03	4e-9	4e-9	8e-9	8.06e-9

The charge of the potassium ion is given in Eq. (14).

$$q^{K^+} = z^{K^+} c^{K^+} F V_{np} \quad (14)$$

where  $z^{K^+}$  is the valence of the potassium ion. We consider  $z^{K^+} = 1$ ,  $c^{K^+}$  is the concentration of the potassium ions.  $F$  is Faraday's constant.

The steady state chlorine ion current in the nanopore is given by Eq. (15).

$$I^{Cl^-} = \frac{q^{Cl^-} u}{L_{np}} + \frac{m^{Cl^-} a u}{\phi} \quad (15)$$

where  $I^{Cl^-}$  is the chlorine ion current,  $q^{Cl^-}$  is the charge of the chlorine ion, and  $m^{Cl^-}$  is the mass of the chlorine ion.

The charge of the chlorine ion is given in Eq. (16).

$$q^{Cl^-} = z^{Cl^-} c^{Cl^-} F V_{np} \quad (16)$$

where  $z^{Cl^-}$  is the valence of the chlorine ion. We consider  $z^{Cl^-} = -1$ ,  $c^{Cl^-}$  is the concentration of the chlorine ion.

The charge of the KCl (q) is given in Eq. (17).

$$q = q^{K^+} + q^{Cl^-} \quad (17)$$

The steady-state ion current in the nanopore is given.

$$I = I^{K^+} + I^{Cl^-}$$

The graphene nanopores do not have a surface charge [13]. In our numerical model, the charge current term  $\frac{qu}{L_{np}}$  contribution is 0.02%. In the graphene nanopore experiments [13], the current oscillations are dependent on the pore diameter only. The KCl salt concentration showed weak dependence on the current oscillations in the graphene nanopore experiments. In our study, the charge obtained from the concentration is small. Table 3 shows the charge of potassium ions and chlorine ions calculated. The charge current of the potassium ions  $\frac{q^{K^+} u}{L_{np}}$  is small. We understand the current in the nanopore has a large electrokinetic contribution from the potential, potassium ion migration, and convective components. The term is  $\frac{m^{K^+} a u}{\phi}$  that contributes to 100% of the potassium ion current in the nanopore. We observe fast mass-only transport from our model. The fast mass transport is observed inside a graphene nanopore [13].

The charge current of chlorine ions  $\frac{q^{Cl^-} u}{L_{np}}$  is small. The electrokinetic term of the chlorine ions  $\frac{m^{Cl^-} a u}{\phi}$  contributes to 100% of the chlorine ions in the nanopore. Our model reduces the computational cost by capturing the effects of the influence of nanopore geometry by volume. We consider the

electrokinetic convective contribution, electric potential, KCl individual potassium ion migration, chlorine ion migration, and charge transport. In order to understand the current oscillations, we go in-depth on the current-time signal [13]. In our analysis, we consider the time step to be 0.05 s. We study for 4 s. The frequency is therefore 0.25 Hz to 20 Hz.

### 3.2. Current oscillations of the nanopore, high-frequency thermal current noise

The high-frequency thermal current noise is given in Eq. (18).

$$I_{high} = \sqrt{4kG_{np}TB} \quad (18)$$

Where  $I_{high}$  is the high-frequency thermal current noise,  $k$  is the Boltzmann constant,  $G_{np}$  is the conductance of the nanopore,  $T$  is the temperature, and  $B$  is the frequency bandwidth in Hz.

The conductance ( $G_{np}$ ) of the nanopore is obtained from Eq. (19).

$$G_{np} = \frac{I}{\phi} \quad (19)$$

Using Eq. (19), we obtain that the conductance in the nanopore is 80 nS. The high-frequency thermal current noise is given in Eq. (18). The value of the high-frequency thermal current noise is small [17].

### Low-frequency charge carrier current noise

The low-frequency charge carrier current noise inside the nanopores is given in Eq. (20).

$$I_{low} = A_{np} f_L \quad (20)$$

where  $I_{low}$  is the low-frequency charge carrier current noise.  $A_{np}$  is the noise property defined by the pore diameter only. We consider the KCl concentration to be 2000 mM [13]. The noise property we call the charge carrier term is given in Eq. (21).

$$A_{np} = \alpha c_{KCl} F V_{np} \quad (21)$$

where  $\alpha$  is the fitting parameter ( $\alpha = 5e6$ ). The noise property  $A_{np}$  is 0.026 nC. The large fitting parameter for graphene to show the charge carrier current noise is consistent with the discussion on the noise inside the graphene nanopores that Hooge's relation has to be revisited in the graphene nanopores [13]. We consider  $f_L$  to be the low-frequency term given in Eq. (22).

$$f_L = 1 / t_L \quad (22)$$

Where  $t_L$  is the time step is 0.05s, to calculate the low-frequency noise. The low frequency  $f_L$  used here is 20 Hz. The noise property  $A_n$  is fixed and oscillates with the time step given. The contribution of the low-frequency charge carrier current noise  $I_{low}$  is 0.52 nA. The contribution of the low-frequency charge carrier current noise and high-frequency thermal current noise to the current inside the nanopore is given in Eq. (23).



$$I_{np} = \begin{cases} I + I_{high} + I_{low}; & \text{oscillation 1} \\ I + I_{high} - I_{low}; & \text{oscillation 2} \end{cases} \quad (23)$$

where  $I_{np}$  are the ion current inside the nanopore that captures the oscillations. Figure 2 shows the current inside the nanopore that matches the literature [13].

### 3.3. Power spectral density (PSD) analysis for the current noise inside the nanopore

We perform the PSD analysis on the current-time numerical simulation for the nanopore. The current-time dynamics of the nanopore are shown in Figure 2. Figure 3 shows the PSD against frequency for the current-time dynamics discussed in Figure 2. The frequency we consider is between 0.01 Hz to 1 Hz. The PSD of the ionic current is calculated using the Welch method [18]. We capture the low-frequency noise scales as  $1/f^s$  with  $s \approx 0.8$ . The nanopore under study is a graphene nanopore [13]. The low frequency  $1/f$  is common for the current-time in graphene nanopores. The  $1/f$  noise in graphene nanopores is due to the pore diameter. The  $1/f$  noise in graphene nanopores has weak dependence on the salt concentration [13]. In our study, we calculate the low-frequency charge carrier current noise from the  $\alpha = 5e6$  parameter. We understand that the charge carrier current noise has a significant volume term. The volume term has the diameter of the graphene nanopore. Hence, we argue that the  $1/f$  noise in graphene nanopores is also due to the pore diameter, similar to the experiments.

### 3.4. Relationship between conductance and solid-state nanopore

We performed the study for nanopore for the thickness of  $L_{np} = 20$  nm and radius 5 nm [12]. We study solid-state nanopores. The ionic conductance ( $G$ ) is related to ionic current ( $I$ ) and applied voltage ( $V$ ). The ionic conductance is given by Eq. (24).

$$G = \frac{I}{V} \quad (24)$$

The ionic conductance inside the nanopore varies significantly compared to the micropore and bulk pore. The nanopore parameters are the geometry that includes length

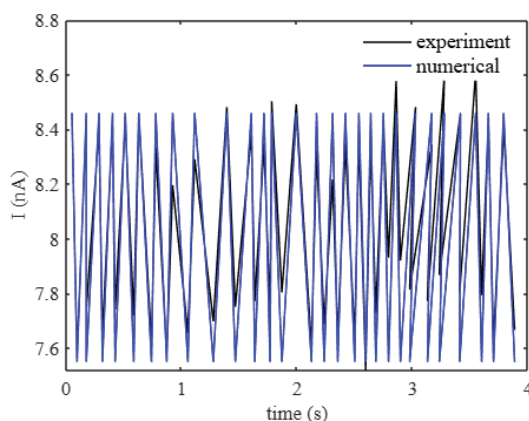


Figure 2: Current oscillations of a nanopore ( $d = 10$  nm) for the applied voltage of 0.1 V. The experiment results of the nanopore are in [13].

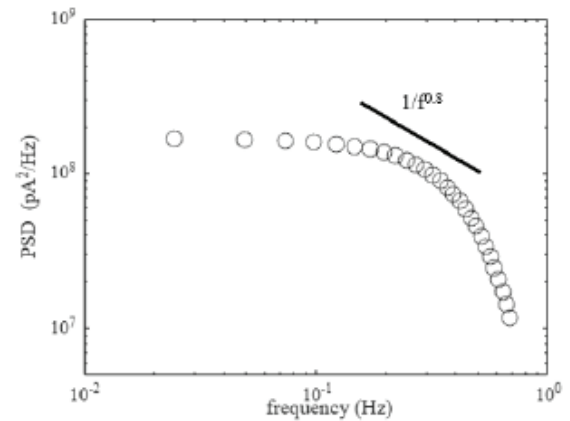


Figure 3: PSD against frequency for the graphene nanopore. The PSD analysis is carried out for the current-time signal considered in Figure 2. The low-frequency  $1/f$  noise in the current is due to the pore diameter.

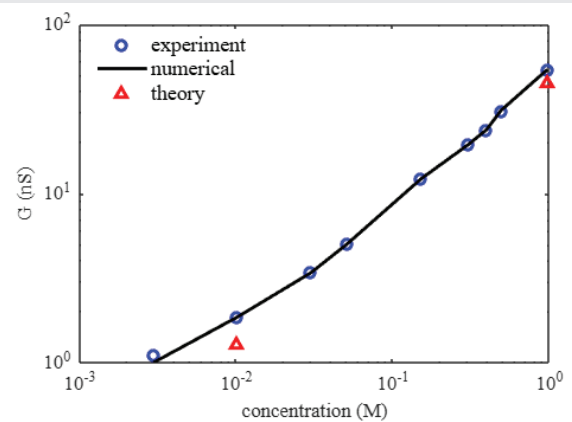


Figure 4: Ionic conductance ( $G$ ) variation with KCl concentration. The blue circles are experiments [12], the black line is numerical, and the red triangles are theory given in Eq. (25).

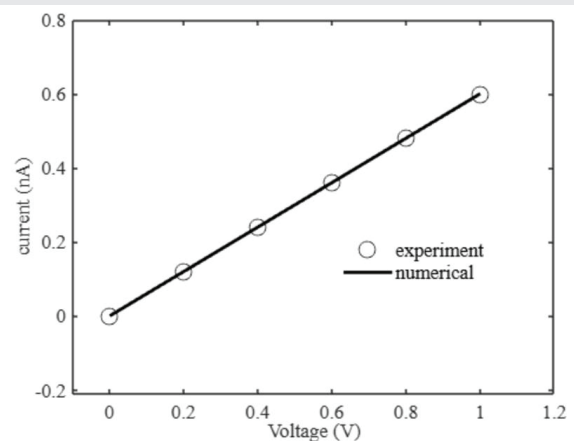


Figure 5: I-V Characteristics for nanopore.

and pore diameter. The surface of the nanopore influences the transport of the KCl. Figure 4 shows the conductance variation with KCl concentration for the nanopore.

We understand the conductance strongly increases with KCl concentration. The conductance is not linear with KCl concentration. This is due to the salt-dependent surface charge

of the nanopore [12]. The existing model given by Eq. (25) captures the conductance variation with the concentration by the pore diameter, volume, and pore geometry [19]. The surface charge is not salt-dependent and is used in the equation with fitting parameters. The term having a surface charge given in terms 1 and term 2 contributes little to the model. The bulk conductivity term  $K_b$  is obtainable [20]. The existing model considers the pore diameter and volume as the dominant contribution to the conductance. The bulk conductivity is the multiplier that changes with KCl concentration, as given in Table 5. Figure 4 shows the conductance for two KCl concentration points only obtained by the model given in Eq. (25).

$$G = K_b \left[ \frac{4L}{\pi d^2} \frac{1}{1 + 4 \left( \frac{l_{Du}}{d} \right)} + \frac{2}{\gamma d + \beta l_{Du}} \right]^{-1} \quad (25)$$

Where  $K_b$  is the bulk conductivity,  $L$  is the pore length, and  $d$  is the pore diameter. We assume the pore diameter is 15 nm.  $l_{Du}$  is the Dukhin length given in Eq. (26).

$$l_{Du} = \left( \frac{\left| \frac{\sigma}{F} \right|}{2c_s} \right) \quad (26)$$

where  $\sigma = 0.7 \text{ mc/m}^2$  is the absolute surface charge density.  $F$  is the Faraday's constant and  $c_s$  is the bulk concentration.  $\gamma$  is a geometrical prefactor fit and  $\beta$  is a fitting parameter (here,  $\gamma = 1$ ,  $\beta = -3$ ) to obtain the best match with the literature [12].

### 3.5. Numerical simulation

We understand the conductance strongly increases with KCl concentration. The conductance is not linear with KCl concentration. We use our numerical simulation to calculate the current inside the nanopore given by Eq. (12) discussed in the earlier section. This is due to the charge term of current  $\frac{qu}{L_{np}}$ .

The charge  $q$  is a function of concentration. The charge  $q$  has the volume of the nanopore. The term  $\frac{mau}{\phi}$  is the electrokinetic term that has the ion mass, ion velocity, acceleration, electric potential, and ion migration.

### 3.6. Smoluchowski model to calculate the velocity of the KCl

The velocity of the KCl inside the nanopore is calculated from the Smoluchowski model given in Eq. (27) [21-23].

$$u = -\mu_E E \quad (27)$$

where  $u$  is the velocity of the KCl inside the nanopore,  $\mu_E$  is the mobility of the KCl inside the nanopore.

$$E = -\frac{\ddot{A}V}{L_{np}} \quad (28)$$

where  $E$  is the electric field inside the nanopore and  $V$  is the applied voltage.  $L_{np}$  is the thickness of the nanopore. The thickness of the nanopore is 20 nm, and the radius is 5 nm. We consider applied voltage = 0.05 V. We consider  $\Delta V = 0.05 \text{ V}$ . The electric field is  $2.5 \times 10^6 \text{ V/m}$ .

### 3.7. Mobility of the potassium chloride electrolyte

$$\mu_E = \frac{\epsilon_{\text{water}} \epsilon_0 \zeta_{\text{membrane}}}{\mu} \quad (29)$$

We consider the surface potential of the membrane having a single nanopore to be 0.052 V [10]. The mobility of the KCl inside the nanopore is  $3.7 \times 10^{-8} \text{ (Am/N)}$ . The velocity of KCl inside the nanopore is 92 mm/s. Table 6 gives the parameters used in the velocity calculations. In this study, for a voltage of 0.05 V,  $u = 0.25 \text{ mm/s}$  is the assumed velocity of the potassium ions, chlorine ions, and KCl inside the nanopore.  $a = 1 \text{ mm/s}^2$  is the assumed acceleration of the potassium ions, chlorine ions, and KCl inside the nanopore.  $m^{K^+} = 5 \times 10^{-6} \text{ kg}$  is the assumed mass of the potassium ions, chlorine ions inside the nanopore. Further, we assume the velocity is varied according to the voltage. Tables 7 to 33 show the conductance and nanopore parameters used in the model for different KCl concentrations. Figure 4 shows the numerical results of the conductance variation with KCl concentration. In our numerical simulation, we observe that the conductance strongly increases with

Table 5: Conductivity variation with KCl concentration [20].

KCl concentration	Conductivity
0.0001 mol/l (0.1 mM)	0.015 mS/cm
0.001 mol/l (1 mM)	0.147 mS/cm
0.01 mol/l (10 mM)	1.41 mS/cm
0.1 mol/l (100 mM)	12.8 mS/cm
1 mol/l (1000 mM)	111 mS/cm

Table 6: Numerical constants and parameter values used in the study.

key parameters	numerical values
relative permittivity of water	80
permittivity of free space	$8.854 \times 10^{-12} \text{ F/m}$
viscosity of the water	$1.003 \times 10^{-3} \text{ Pa.s}$
Faraday constant	96485.3 C/mol
gas constant	8.314 J/(mol K)
Avogadro number	$6.023 \times 10^{23} \text{ mol}^{-1}$
Boltzmann constant	$1.38 \times 10^{-23} \text{ J/K}$
electronic charge	$1.602 \times 10^{-19} \text{ C}$
Temperature	300 K

Table 7: Conductance and nanopore list 1 model parameters. The concentration of KCl is 3 mM.

$\phi(V)$	$V_{np} (m^3)$	$c^{Cl^-} (mM)$	$m^{K^+} (kg)$	$m^{Cl^-} (kg)$	$q^{K^+} (C)$	$q^{Cl^-} (C)$	$q^{CT} (C)$
0.05	1.57E-24	3	3	5.00E-06	5.00E-06	4.43E-19	-4.43E-19
0.1	1.57E-24	3	3	5.00E-06	5.00E-06	4.43E-19	-4.43E-19
0.15	1.57E-24	3	3	5.00E-06	5.00E-06	4.43E-19	-4.43E-19
0.2	1.57E-24	3	3	5.00E-06	5.00E-06	4.43E-19	-4.43E-19

KCl concentration. The conductance is not linear with KCl concentration. We account for the salt-dependent charge of the nanopore, pore diameter, pore thickness, pore geometry, pore volume, electric potential, electrokinetic term, ion mass, ion migration, ion velocity, acceleration, charge transport, and convective contribution in our numerical simulation. We could understand the experimental observations in our numerical simulation [12].

### 3.8. Influence of the transport of the ion in the solid-state nanopore

Here we study the linear current-voltage inside the solid state nanopore [24]. We consider a nanopore of thickness 10

**Table 8:** Conductance and nanopore list 2 model parameters. The concentration of KCl is 3 mM.

$v$ (m/s)	$a$ (m/s <sup>2</sup> )	$I^{K^+}$ (A)	$I^{Cl^-}$ (A)	$I$ (A) (numerical)	$I$ (A) (experiment)
2.50E-04	1.00E-03	2.50E-11	2.50E-11	5.00E-11	5.10E-11
1.00E-03	1.00E-03	5.00E-11	5.00E-11	1.00E-10	1.00E-10
2.30E-03	1.00E-03	7.67E-11	7.67E-11	1.53E-10	1.50E-10
4.30E-03	1.00E-03	1.08E-10	1.08E-10	2.15E-10	2.00E-10

**Table 9:** Conductance and nanopore list 3 model parameters. The concentration of KCl is 3 mM.

Conductance (S) (numerical)	Conductance (S) (experiments)
1e-9	1E-09
1e-9	1E-09
1.02e-9	1E-09
1.08e-9	1E-09

**Table 10:** Conductance and nanopore list 4 model parameters. The concentration of KCl is 10 mM.

$\phi$ (V)	$V_{ap}$ (m <sup>3</sup> )	$c^{Cl^-}$ (mM)	$m^{K^+}$ (kg)	$m^{Cl^-}$ (kg)	$q^{K^+}$ (C)	$q^{Cl^-}$ (C)	$q^{Cl^-}$ (C)
0.05	1.57E-24	10	10	1.70E-05	1.70E-05	1.52E-18	-1.52E-18
0.1	1.57E-24	10	10	1.70E-05	1.70E-05	1.52E-18	-1.52E-18
0.15	1.57E-24	10	10	1.70E-05	1.70E-05	1.52E-18	-1.52E-18
0.2	1.57E-24	10	10	1.70E-05	1.70E-05	1.52E-18	-1.52E-18

**Table 11:** Conductance and nanopore list 5 model parameters. The concentration of KCl is 10 mM.

$v$ (m/s)	$a$ (m/s <sup>2</sup> )	$I^{K^+}$ (A)	$I^{Cl^-}$ (A)	$I$ (A) (numerical)	$I$ (A) (experiment)
1.40E-04	1.00E-03	4.76E-11	4.76E-11	9.52E-11	9.30E-11
5.50E-04	1.00E-03	9.35E-11	9.35E-11	1.87E-10	1.86E-10
1.25E-03	1.00E-03	1.42E-10	1.42E-10	2.84E-10	2.79E-10
2.20E-03	1.00E-03	1.87E-10	1.87E-10	3.74E-10	3.72E-10

**Table 12:** Conductance and nanopore list 6 model parameters. The concentration of KCl is 10 mM.

Conductance (S) (numerical)	Conductance (S) (experiments)
1.90E-09	1.86E-09
1.87E-09	1.86E-09
1.89E-09	1.86E-09
1.87E-09	1.86E-09

**Table 13:** Conductance and nanopore list 7 model parameters. The concentration of KCl is 30 mM.

$\phi$ (V)	$V_{ap}$ (m <sup>3</sup> )	$c^{Cl^-}$ (mM)	$m^{K^+}$ (kg)	$m^{Cl^-}$ (kg)	$q^{K^+}$ (C)	$q^{Cl^-}$ (C)	$q^{Cl^-}$ (C)
0.05	1.57E-24	30	30	5.00E-05	5.00E-05	4.54446E-18	-4.54446E-18
0.1	1.57E-24	30	30	5.00E-05	5.00E-05	4.54446E-18	-4.54446E-18
0.15	1.57E-24	30	30	5.00E-05	5.00E-05	4.54446E-18	-4.54446E-18
0.2	1.57E-24	30	30	5.00E-05	5.00E-05	4.54446E-18	-4.54446E-18

**Table 14:** Conductance and nanopore list 8 model parameters. The concentration of KCl is 30 mM.

$v$ (m/s)	$a$ (m/s <sup>2</sup> )	$I^{K^+}$ (A)	$I^{Cl^-}$ (A)	$I$ (A) (numerical)	$I$ (A) (experiment)
8.50E-05	1.00E-03	8.50E-11	8.50E-11	1.70E-10	1.70E-10
3.40E-04	1.00E-03	1.70E-10	1.70E-10	3.40E-10	3.40E-10
7.70E-04	1.00E-03	2.57E-10	2.57E-10	5.14E-10	5.10E-10
1.35E-03	1.00E-03	3.38E-10	3.38E-10	6.76E-10	6.80E-10

**Table 15:** Conductance and nanopore list 9 model parameters. The concentration of KCl is 30 mM.

Conductance (S) (numerical)	Conductance (S) (experiments)
3.40E-09	3.40E-09
3.40E-09	3.40E-09
3.42E-09	3.40E-09
3.38E-09	3.40E-09

**Table 16:** Conductance and nanopore list 10 model parameters. The concentration of KCl is 50 mM.

$\phi$ (V)	$V_{ap}$ (m <sup>3</sup> )	$c^{Cl^-}$ (mM)	$m^{K^+}$ (kg)	$m^{Cl^-}$ (kg)	$q^{K^+}$ (C)	$q^{Cl^-}$ (C)	$q^{Cl^-}$ (C)
0.05	1.57E-24	50	50	8.50E-05	8.50E-05	7.5741E-18	-7.5741E-18
0.1	1.57E-24	50	50	8.50E-05	8.50E-05	7.5741E-18	-7.5741E-18
0.15	1.57E-24	50	50	8.50E-05	8.50E-05	7.5741E-18	-7.5741E-18
0.2	1.57E-24	50	50	8.50E-05	8.50E-05	7.5741E-18	-7.5741E-18

**Table 17:** Conductance and nanopore list 11 model parameters. The concentration of KCl is 50 mM.

$v$ (m/s)	$a$ (m/s <sup>2</sup> )	$I^{K^+}$ (A)	$I^{Cl^-}$ (A)	$I$ (A) (numerical)	$I$ (A) (experiment)
7.30E-05	1.00E-03	1.24E-10	1.24E-10	2.48E-10	2.50E-10
3.00E-04	1.00E-03	2.55E-10	2.55E-10	5.10E-10	5.00E-10
6.50E-04	1.00E-03	3.69E-10	3.69E-10	7.37E-10	7.50E-10
1.20E-03	1.00E-03	5.10E-10	5.10E-10	1.02E-09	1.00E-09

**Table 18:** Conductance and nanopore list 12 model parameters. The concentration of KCl is 50 mM.

Conductance (S) (numerical)	Conductance (S) (experiments)
4.97E-09	5.00E-09
5.10E-09	5.00E-09
4.91E-09	5.00E-09
5.10E-09	5.00E-09

nm and radius 0.5 nm. We study 1 M KCl. The reason for the linear I-V characteristics is due to the pore diameter, pore thickness, and pore geometry, charge, surface charge of the nanopore, concentration, and ion mobility [24]. The experiment

**Table 19:** Conductance and nanopore list 13 model parameters. The concentration of KCl is 150 mM.

$\phi$ (V)	$V_{np}$ (m <sup>3</sup> )	$c^{CT}$ (mM)	$m^{K^+}$ (kg)	$m^{Cl^-}$ (kg)	$q^{K^+}$ (C)	$q^{Cl^-}$ (C)	$q^{CT}$ (C)
0.05	1.57E-24	150	150	2.60E-04	2.60E-04	2.27223E-17	-2.27223E-17
0.1	1.57E-24	150	150	2.60E-04	2.60E-04	2.27223E-17	-2.27223E-17
0.15	1.57E-24	150	150	2.60E-04	2.60E-04	2.27223E-17	-2.27223E-17
0.2	1.57E-24	150	150	2.60E-04	2.60E-04	2.27223E-17	-2.27223E-17

**Table 20:** Conductance and nanopore list 14 model parameters. The concentration of KCl is 150 mM.

$v$ (m/s)	$a$ (m/s <sup>2</sup> )	$I^{K^+}$ (A)	$I^{Cl^-}$ (A)	$I$ (A) (numerical)	$I$ (A) (experiment)
6.00E-05	1.00E-03	3.12E-10	3.12E-10	6.24E-10	6.15E-10
2.30E-04	1.00E-03	5.98E-10	5.98E-10	1.20E-09	1.23E-09
5.30E-04	1.00E-03	9.19E-10	9.19E-10	1.84E-09	1.85E-09
9.70E-04	1.00E-03	1.26E-09	1.26E-09	2.52E-09	2.50E-09

**Table 21:** Conductance and nanopore list 15 model parameters. The concentration of KCl is 150 mM.

Conductance (S) (numerical)	Conductance (S) (experiments)
1.25E-08	1.23E-08
1.20E-08	1.23E-08
1.23E-08	1.23E-08
1.26E-08	1.23E-08

**Table 22:** Conductance and nanopore list 16 model parameters. The concentration of KCl is 300 mM.

$\phi$ (V)	$V_{np}$ (m <sup>3</sup> )	$c^{CT}$ (mM)	$m^{K^+}$ (kg)	$m^{Cl^-}$ (kg)	$q^{K^+}$ (C)	$q^{Cl^-}$ (C)	$q^{CT}$ (C)
0.05	1.57E-24	300	300	5.00E-04	5.00E-04	4.54446E-17	-4.5E-17
0.1	1.57E-24	300	300	5.00E-04	5.00E-04	4.54446E-17	-4.5E-17
0.15	1.57E-24	300	300	5.00E-04	5.00E-04	4.54446E-17	-4.5E-17
0.2	1.57E-24	300	300	5.00E-04	5.00E-04	4.54446E-17	-4.5E-17

**Table 23:** Conductance and nanopore list 17 model parameters. The concentration of KCl is 300 mM.

$v$ (m/s)	$a$ (m/s <sup>2</sup> )	$I^{K^+}$ (A)	$I^{Cl^-}$ (A)	$I$ (A) (numerical)	$I$ (A) (experiment)
4.90E-05	1.00E-03	4.90E-10	4.90E-10	9.80E-10	9.75E-10
1.95E-04	1.00E-03	9.75E-10	9.75E-10	1.95E-09	1.95E-09
4.10E-04	1.00E-03	1.37E-09	1.37E-09	2.73E-09	2.93E-09
7.80E-04	1.00E-03	1.95E-09	1.95E-09	3.90E-09	3.90E-09

**Table 24:** Conductance and nanopore list 18 model parameters. The concentration of KCl is 300 mM.

Conductance (S) (numerical)	Conductance (S) (experiments)
1.96E-08	1.95E-08
1.95E-08	1.95E-08
1.82E-08	1.95E-08
1.95E-08	1.95E-08

**Table 25:** Conductance and nanopore list 19 model parameters. The concentration of KCl is 400 mM.

$\phi$ (V)	$V_{np}$ (m <sup>3</sup> )	$c^{CT}$ (mM)	$m^{K^+}$ (kg)	$m^{Cl^-}$ (kg)	$q^{K^+}$ (C)	$q^{Cl^-}$ (C)	$q^{CT}$ (C)
0.05	1.57E-24	400	400	6.50E-04	6.50E-04	6.05928E-17	-6.05928E-17
0.1	1.57E-24	400	400	6.50E-04	6.50E-04	6.05928E-17	-6.05928E-17
0.15	1.57E-24	400	400	6.50E-04	6.50E-04	6.05928E-17	-6.05928E-17
0.2	1.57E-24	400	400	6.50E-04	6.50E-04	6.05928E-17	-6.05928E-17

**Table 26:** Conductance and nanopore list 20 model parameters. The concentration of KCl is 400 mM.

$v$ (m/s)	$a$ (m/s <sup>2</sup> )	$I^{K^+}$ (A)	$I^{Cl^-}$ (A)	$I$ (A) (numerical)	$I$ (A) (experiment)
4.70E-05	1.00E-03	6.11E-10	6.11E-10	1.22E-09	1.20E-09
1.85E-04	1.00E-03	1.20E-09	1.20E-09	2.41E-09	2.40E-09
4.10E-04	1.00E-03	1.78E-09	1.78E-09	3.56E-09	3.50E-09
7.20E-04	1.00E-03	2.34E-09	2.34E-09	4.68E-09	4.80E-09

**Table 27:** Conductance and nanopore list 21 model parameters. The concentration of KCl is 400 mM.

Conductance (S) (numerical)	Conductance (S) (experiments)
2.44E-08	2.38E-08
2.41E-08	2.38E-08
2.37E-08	2.38E-08
2.34E-08	2.38E-08

**Table 28:** Conductance and nanopore list 22 model parameters. The concentration of KCl is 500 mM.

$\phi$ (V)	$V_{np}$ (m <sup>3</sup> )	$c^{CT}$ (mM)	$m^{K^+}$ (kg)	$m^{Cl^-}$ (kg)	$q^{K^+}$ (C)	$q^{Cl^-}$ (C)	$q^{CT}$ (C)
0.05	1.57E-24	500	500	8.50E-04	8.50E-04	7.5741E-17	-7.5741E-17
0.1	1.57E-24	500	500	8.50E-04	8.50E-04	7.5741E-17	-7.5741E-17
0.15	1.57E-24	500	500	8.50E-04	8.50E-04	7.5741E-17	-7.5741E-17
0.2	1.57E-24	500	500	8.50E-04	8.50E-04	7.5741E-17	-7.5741E-17

**Table 29:** Conductance and nanopore list 23 model parameters. The concentration of KCl is 500 mM.

$v$ (m/s)	$a$ (m/s <sup>2</sup> )	$I^{K^+}$ (A)	$I^{Cl^-}$ (A)	$I$ (A) (numerical)	$I$ (A) (experiment)
4.60E-05	1.00E-03	7.82E-10	7.82E-10	1.56E-09	1.55E-09
1.82E-04	1.00E-03	1.55E-09	1.55E-09	3.10E-09	3.10E-09
4.10E-04	1.00E-03	2.32E-09	2.32E-09	4.65E-09	4.65E-09
7.30E-04	1.00E-03	3.11E-09	3.11E-09	6.21E-09	6.20E-09

**Table 30:** Conductance and nanopore list 24 model parameters. The concentration of KCl is 500 mM.

Conductance (S) (numerical)	Conductance (S) (experiments)
3.13E-08	3.10E-08
3.10E-08	3.10E-08
3.10E-08	3.10E-08
3.11E-08	3.10E-08



**Table 31:** Conductance and nanopore list 25 model parameters. The concentration of KCl is 1000 mM.

$\phi$ (V)	$V_{np}$ (m <sup>3</sup> )	$c^{CT}$ (mM)	$m^{K^+}$ (kg)	$m^{Cl^-}$ (kg)	$q^{K^+}$ (C)	$q^{Cl^-}$ (C)	$q^{CT}$ (C)
0.05	1.57E-24	1000	1000	1.70E-03	1.70E-03	1.51482E-16	-1.51482E-16
0.1	1.57E-24	1000	1000	1.70E-03	1.70E-03	1.51482E-16	-1.51482E-16
0.15	1.57E-24	1000	1000	1.70E-03	1.70E-03	1.51482E-16	-1.51482E-16
0.2	1.57E-24	1000	1000	1.70E-03	1.70E-03	1.51482E-16	-1.51482E-16

**Table 32:** Conductance and nanopore list 26 model parameters. The concentration of KCl is 1000 mM.

$v$ (m/s)	$a$ (m/s <sup>2</sup> )	$I^{K^+}$ (A)	$I^{Cl^-}$ (A)	$I$ (A) (numerical)	$I$ (A) (experiment)
4.00E-05	1.00E-03	1.36E-09	1.36E-09	2.72E-09	2.70E-09
1.60E-04	1.00E-03	2.72E-09	2.72E-09	5.44E-09	5.40E-09
3.60E-04	1.00E-03	4.08E-09	4.08E-09	8.16E-09	8.10E-09
6.40E-04	1.00E-03	5.44E-09	5.44E-09	1.09E-08	1.08E-08

**Table 33:** Conductance and nanopore list 27 model parameters. The concentration of KCl is 1000 mM.

Conductance (S) (numerical)	Conductance (S) (experiments)
5.44E-08	5.40E-08
5.44E-08	5.40E-08
5.44E-08	5.40E-08
5.44E-08	5.40E-08

**Table 34:** Conductance and nanopore [24] list 1 model parameters. The concentration of KCl is 1000 mM.

$\phi$ (V)	$V_{np}$ (m <sup>3</sup> )	$c^{CT}$ (mM)	$m^{K^+}$ (kg)	$m^{Cl^-}$ (kg)	$q^{K^+}$ (C)	$q^{Cl^-}$ (C)	$q^{CT}$ (C)
0.2	7.85E-27	1000	1000	1.70E-03	1.70E-03	7.57E-19	-7.57E-19
0.4	7.85E-27	1000	1000	1.70E-03	1.70E-03	7.57E-19	-7.57E-19
0.6	7.85E-27	1000	1000	1.70E-03	1.70E-03	7.57E-19	-7.57E-19
0.8	7.85E-27	1000	1000	1.70E-03	1.70E-03	7.57E-19	-7.57E-19
1	7.85E-27	1000	1000	1.70E-03	1.70E-03	7.57E-19	-7.57E-19

**Table 35:** Conductance and nanopore [24] list 2 model parameters. The concentration of KCl is 1000 mM.

$v$ (m/s)	$a$ (m/s <sup>2</sup> )	$I^{K^+}$ (A)	$I^{Cl^-}$ (A)	$I$ (A) (numerical)	$I$ (A) (experiment)
7.50E-06	1.00E-03	6.21E-11	6.21E-11	1.24E-10	1.25E-10
3.00E-05	1.00E-03	1.25E-10	1.25E-10	2.50E-10	2.60E-10
6.30E-05	1.00E-03	1.80E-10	1.80E-10	3.59E-10	3.60E-10
1.15E-04	1.00E-03	2.45E-10	2.45E-10	4.90E-10	4.90E-10
1.85E-04	1.00E-03	3.15E-10	3.15E-10	6.29E-10	6.30E-10

**Table 36:** Conductance and nanopore [24] list 3 model parameters. The concentration of KCl is 1000 mM.

Conductance numerical (S)	conductance experiments (S)
6.05E-10	6.30E-10
6.15E-10	6.30E-10
6.03E-10	6.30E-10
6.14E-10	6.30E-10
6.29E-10	6.30E-10

nanopore considered is silicon nitride. The surface potential of the silicon nitride is unknown. Tables 34 to 37 show the parameters used in our numerical simulation to match the I-V characteristics given in the literature [24]. In our simulation, the pore diameter is 1 nm, the pore thickness is 10 nm, and the pore geometry we consider is volume ( $V_{np}$ ) only. We calculate the charge from concentration, volume, Faraday's constant, and valence of KCl. We separate the contribution of mobility and ion mass. We assume the ion mass. We assume the ion velocities that are reasonable in the nanopore [22,23] due to the unknown parameter surface potential of the silicon nitride nanoporous membrane. The parameter surface potential, in combination with the Smoluchowski model, gives the velocity of the ions as given in the earlier section. The surface charge can be obtained from the surface potential the Coulomb's law. We consider a 1 M KCl concentration. The ion mobility gives the ion velocity in the Smoluchowski equation as given in the earlier section. In our study, we consider the current contribution from the charge term and the electrokinetic term, having the ion mass as discussed in the earlier section. Our model reduces the computational cost. Our model accounts for most of the discussions given in the literature [24] to understand the I-V characteristics in solid-state nanopores. In the future, we have to understand the surface potential for the silicon nitride nanoporous membrane to improve our model. Figure 5 shows the current-voltage simulation for the nanopore. We observe linear I-V characteristics for 1 M KCl inside the nanopore. The conductance for 1 M KCl inside the nanopore is 0.62 nS, which matches the literature [24].

## 4. Conclusion

In this paper, we study using low computational cost numerical simulation for ion transport inside the nanopores and conical nanopores. We study the current-time, 1/f low-frequency noise, conductance variation with the concentration, current-voltage in nanopores, and studies in conical nanopores. We found that current noise is present inside the nanopores and conical nanopores. The study should help to understand solid-state nanoporous membranes for energy, water desalination, DNA sequencing, and neuromorphic computing applications.

## References

1. Siria A, Poncharal P, Bianco AL, Fulcrand R, Blase X, Purcell ST, et al. Giant osmotic energy conversion measured in a single nanopore boron nitride nanotube. *Nature*. 2013 Feb 21;494(7438):455–8. Available from: <https://doi.org/10.1038/nature11876>
2. Lee C, Joly L, Siria A, Bianco AL, Fulcrand R, Bocquet L. Large apparent electric size of solid-state nanopores due to spatially extended surface conduction. *Nano Lett*. 2012 Aug 8;12(8):4037–44. Available from: <https://doi.org/10.1021/nl301412b>
3. Feng J, Graf M, Liu K, Ovchinnikov D, Dumcenco D, Heiranian M, et al. Single-layer MoS2 nanopores as nanopower generators. *Nature*. 2016 Aug 11;536(7615):197–200. Available from: <https://doi.org/10.1038/nature18593>
4. Emmerich T, Vasu KS, Niguès A, Keerthi A, Radha B, Siria A, et al. Enhanced nanofluidic transport in activated carbon nanoconduits. *Nat Mater*. 2022 Jun;21(6):696–702. Available from: <https://doi.org/10.1038/s41563-022-01229-x>

5. Rankin DJ, Bocquet L, Huang DM. Entrance effects in concentration-gradient-driven flow through an ultrathin porous membrane. *J Chem Phys*. 2019 Jul 29;151(4):044705. Available from: <https://doi.org/10.1063/1.5108700>
6. Balme S, Picaud F, Manghi M, Palmeri J, Bechelany M, Cabello-Aguilar S, et al. Ionic transport through sub-10 nm diameter hydrophobic high-aspect ratio nanopores: experiment, theory and simulation. *Sci Rep*. 2015 Jun 3;5:10135. Available from: <https://doi.org/10.1038/srep10135>
7. Jain T, Rasera BC, Guerrero RJ, Boutilier MS, O'Hern SC, Idrobo JC, et al. Heterogeneous sub-continuum ionic transport in statistically isolated graphene nanopores. *Nat Nanotechnol*. 2015 Dec;10(12):1053–7. Available from: <https://doi.org/10.1038/nnano.2015.222>
8. Wang H, Nandigana VVR, Jo KD, Aluru NR, Timperman AT. Controlling the ionic current rectification factor of a nanofluidic/microfluidic interface with symmetric nanocapillary interconnects. *Anal Chem*. 2015 Mar 17;87(6):3598–605. Available from: <https://doi.org/10.1021/ac5019638>
9. Nandigana VVR, Jo K, Timperman A, Aluru NR. Asymmetric-fluidic-reservoirs induced high rectification nanofluidic diode. *Sci Rep*. 2018 Sep 17;8:13941. Available from: <https://doi.org/10.1038/s41598-018-32284-7>
10. Ragulranjith SK, Nandigana VVR. Membrane measurement, device simulations of nanochannel, nanopore and nanofluidics electronics calculator. *Trans Eng Comput Sci*. 2025;13:1–61. Available from: <https://doi.org/10.14738/tmlai.1304.19127>
11. Forni T, Baldoni M, Piane FL, Mercuri F. GrapheNet: a deep learning framework for predicting the physical and electronic properties of nanographenes using images. *Sci Rep*. 2024;14:24576. Available from: <https://doi.org/10.1038/s41598-024-75841-z>
12. Smeets RMM, Keyser UF, Dekker NH, Dekker C. Noise in solid-state nanopores. *Proc Natl Acad Sci U S A*. 2008 Jan 15;105(2):417–21. Available from: <https://doi.org/10.1073/pnas.0705349105>
13. Heerema SJ, Schneider GF, Rozemuller M, Vicarelli L, Zandbergen HW, Dekker C. 1/f noise in graphene nanopores. *Nanotechnology*. 2015 Feb 20;26(7):074001. Available from: <https://doi.org/10.1088/0957-4484/26/7/074001>
14. Feng J, Liu K, Graf M, Dumcenco D, Kis A, Di Ventra M, et al. Observation of ionic Coulomb blockade in nanopores. *Nat Mater*. 2016 Aug;15(8):850–5. Available from: <https://doi.org/10.1038/nmat4607>
15. Powell MR, Martens C, Siwy ZS. Asymmetric properties of ion current 1/f noise in conically shaped nanopores. *Chem Phys*. 2010 Aug 7;375(2–3):529–35. Available from: <https://doi.org/10.1016/j.chemphys.2010.06.008>
16. Portillo S, Ramirez P, Mafe S, Cervera J. Neuromorphic reservoir computing with memristive nanofluidic diodes. *Nano Lett*. 2025;25(11):9928–34. Available from: <https://doi.org/10.1021/acs.nanolett.5c00853>
17. Keithley Digital Multimeter, Bench, 6.5 Digit, DMM6500. Industry Buying, India. Available from: <https://www.industrybuying.com/digital-multimeters-keithley-TES.DIG.932431721>
18. Welch D. The use of fast Fourier transform for the estimation of power spectra: a method based on time averaging over short, modified periodograms. *IEEE Trans Audio Electroacoust*. 1967;15(2):70–3. Available from: [https://barnes.atmos.colostate.edu/COURSES/AT655\\_S15/references/Welch\\_1967\\_IEETransAudioElect.pdf](https://barnes.atmos.colostate.edu/COURSES/AT655_S15/references/Welch_1967_IEETransAudioElect.pdf)
19. Patil O, Manikandan D, Nandigana VVR. A molecular dynamics simulation framework for predicting noise in solid-state nanopores. *Mol Simul*. 2020;46(12):1011–6. Available from: <http://dx.doi.org/10.1080/08927022.2020.1798004>
20. Merck. Available from: <https://www.sigmaaldrich.com/>
21. Schoch RB, Han J, Renaud P. Transport phenomena in nanofluidics. *Rev Mod Phys*. 2008 Jul 16;80(3):839–83. Available from: <https://doi.org/10.1103/RevModPhys.80.839>
22. Pennathur S, Santiago JG. Electrokinetic transport in nanochannels. 1. Theory. *Anal Chem*. 2005 Oct 1;77(21):6772–81. Available from: <https://doi.org/10.1021/ac050835y>
23. Pennathur S, Santiago JG. Electrokinetic transport in nanochannels. 2. Experiments. *Anal Chem*. 2005 Oct 1;77(21):6782–9. Available from: <https://doi.org/10.1021/ac0508346>
24. Ho C, Qiao R, Heng JB, Chatterjee A, Timp RJ, Aluru NR, et al. Electrolytic transport through a synthetic nanometer-diameter pore. *Proc Natl Acad Sci U S A*. 2005 Jul 26;102(30):10445–50. Available from: <https://doi.org/10.1073/pnas.0500796102>

## Discover a bigger Impact and Visibility of your article publication with Peertechz Publications

### Highlights

- ❖ Signatory publisher of ORCID
- ❖ Signatory Publisher of DORA (San Francisco Declaration on Research Assessment)
- ❖ Articles archived in worlds' renowned service providers such as Portico, CNKI, AGRIS, TDNet, Base (Bielefeld University Library), CrossRef, Scilit, J-Gate etc.
- ❖ Journals indexed in ICMJE, SHERPA/ROMEO, Google Scholar etc.
- ❖ OAI-PMH (Open Archives Initiative Protocol for Metadata Harvesting)
- ❖ Dedicated Editorial Board for every journal
- ❖ Accurate and rapid peer-review process
- ❖ Increased citations of published articles through promotions
- ❖ Reduced timeline for article publication

Submit your articles and experience a new surge in publication services

<https://www.peertechzpublications.org/submission>

Peertechz journals wishes everlasting success in your every endeavours.